A Physics- and Chemistry-Informed Neural Network for Simulating Mine Waste Weathering: Application to Pyrite Oxidation Modeling

Hanli Qiao[1], Mohammad Jooshaki[1], Massimo Rolle[2], Timo Lähivaara[3], Marko Vauhkonen[3], Tommi Kauppila[1], Muhammad Muniruzzaman[1,4]

[1]*Geological Survey of Finland, Vuorimiehentie 5, 02151, Espoo, Finland*

[2]*Institute of Applied Geosciences, Technical University of Darmstadt, Schnittspahnstraße 9, 64287, Darmstadt, Germany*

[3]*Department of Technical Physics, University of Eastern Finland, Yliopistonranta 1, 70211, Kuopio, Finland*

[4]*Institute of Geosciences, University of Bonn, Kirschallee 1–3, 53115 Bonn, Germany*

Abstract

Mining environments involve complex hydro-bio-geochemical systems. Reactive transport modeling (RTM) is essential to rigorously describe these processes. Yet, process-based RTM is computationally intensive and limited in practical applications. To mitigate such challenges, this paper provides a novel deep learning-based surrogate accelerator, hidden-reactive-transport-neural-network (HRTNet), to simulate pyrite oxidation, a process of key importance for acid mine drainage. HRTNet relies on a flexible two-network architecture integrating chemical and physical equations. The model can effectively capture the desired spatio-temporal dynamics in a considerably reduced computation time (almost eight-fold). Additionally, HRTNet shows a good generalization capability covering a wide range of conditions beyond the training datasets.

Keywords: Mine waste weathering, machine learning, physics-chemistry-informed neural network, pyrite oxidation, reactive transport modeling

Introduction

In mining settings, intricate geochemical and hydrogeological conditions interact at multiple scales. These systems usually involve mineral dissolution and precipitation, contaminant release and transport, gaseous species migration, and the eventual formation of acid mine drainage (AMD), which poses a severe pollution issue due to high concentrations of sulfate, elements of potential concern such as metals and metalloids, and low pH. The oxidation of sulfide minerals is one of the primary sources of AMD, where pyrite and pyrrhotite are principal minerals that generate acidic drainage in mine waste (Moncur *et al.* 2009; Kefeni *et al.* 2017; Simate and Ndlovu 2014). Pyrite oxidation is thus a main driver of the environmental and economical challenges associated with AMD (Chandra and Gerson 2010). Effectively capturing the dynamics of these processes enables accurate prediction and monitoring of their environmental influences, thereby facilitating mitigation of pollution risks. Reactive transport modeling (RTM) is a sophisticated approach that can resolve these coupled processes, by integrating a wide range of physical, chemical, and biological processes in mining waste and mining-affected subsurface systems (Steefel *et al.* 2005; Xu *et al.* 2000; Battistel *et al.* 2019; 2021).

While these process-based models are accurate and represent a rigorous formulation, they are often computationally intensive, resulting in limitations in many practical applications that require multiple model-based evaluations and risk assessments (Steefel 2019; Muniruzzaman and Pedretti, 2021). These challenges

mainly stem from the demand for solving a suite of highly coupled partial differential equations (PDEs). In recent years, numerous efforts have been devoted to mitigating the computational burden associated with the process-based RTM simulations, with surrogate models presenting promising potentials. Among these techniques, machine learning (ML) and deep learning (DL) based accelerators have received increasing attention, including successful applications in geochemical calculations (Jatnieks *et al.* 2016; Laloy and Jacques 2022; Demirer *et al.* 2023; Guérillot and Bruyelle 2020; Leal *et al.* 2020), parameter upscaling (Prasianakis *et al.* 2020), and uncertainty and sensitivity analysis (Degen *et al.* 2022). So far, purely data-driven surrogate models have been the primary approach in diverse geochemical and transport problems like in hyporheic zone (Moeini *et al.* 2024), electrokinetic transport (Sprocati and Rolle 2021; Sprocati *et al.* 2025), dolomitization process (Li *et al.* 2022), porous media transport (Marcato *et al.* 2023), and riparian zone (Yu *et al.* 2024). Unlike fully data-driven models, strategies combining geochemical or physical knowledge were developed to improve prediction accuracy while promising large speedups. These formulations consider governing knowledge either as a priori (De Lucia 2024) or a trigger of fully physical simulation when the surrogate predictions are implausible (De Lucia and Kühn 2021). Additionally, physics-based ML is another model that has been developed for geoscientific systems by integrating the solutions of the governing PDEs and data-driven methods using the non-intrusive reduced-basis model (Degen *et al.* 2023). Finally, physics-informed ML (PIML) has been a promising technique, which explicitly integrates governing physical laws into the learning process. This can be achieved by embedding PDE residuals in the loss function, as demonstrated by Raissi *et al.* (2019) in their work on physics-informed neural networks (PINNs), or by encoding these laws directly into the neural network architecture (Rao *et al.* 2023; Liu *et al.* 2024).

Recently, PIML techniques have been successfully applied in various systems, yet contributions to accelerating process-based RTM are still scarce and require systematic studies. The work in this paper aims to contribute to this research gap. The study was inspired by the Hidden Fluid Mechanics (HFM) model provided by Raissi *et al.* (2020) to propose an intelligent surrogate model, the Hidden Reactive Transport Neural Network (HRTNet), which integrates the governing physical and chemical reaction laws. To this end, HRTNet is applied and tested for pyrite oxidation examples to evaluate its performance. HRTNet results were compared against the process-based RTM simulations to assess the accuracy and generalization capability of the proposed surrogate modelling approach.

Methods

We consider the study by Battistel *et al.* (2019) as a model problem, relevant for mine waste weathering processes, for investigating pyrite oxidation reactive fronts in 1-D and 2-D porous media. The left panel in Fig. 1 shows the 1-D and 2-D flow-through experiments described by Battistel *et al.* (2019). In 1-D case, a cylindrical glass column was used, where a pyrite inclusion (4 cm long, placed in the middle, with 67.63 mol/Lwater pyrite) was embedded within a sandy matrix. In contrast, a quasi two-dimensional flow-through chamber, packed with a sandy matrix containing a rectangular pyrite inclusion (located at 5 cm from the inlet and 10 cm from bottom, with 33.82 mol/Lwater pyrite), was used for the 2-D experiment. These experiments were performed by continuously injecting an oxic solution, and a non-invasive optode technique was used to monitor oxygen front propagation at high-spatial and temporal resolution. O_2 sensor strips adhered to the inner walls of the flow-through setups are shown in pink color in Fig. 1. A physically homogeneous but chemically and mineralogically heterogeneous system is generated by keeping the same grain sizes of the sand and pyrite.

We leverage the same process-based RTM as used by Battistel *et al.* (2019) to simulate the 1-D and 2-D flow-through experiments. The model is a basis for generating the

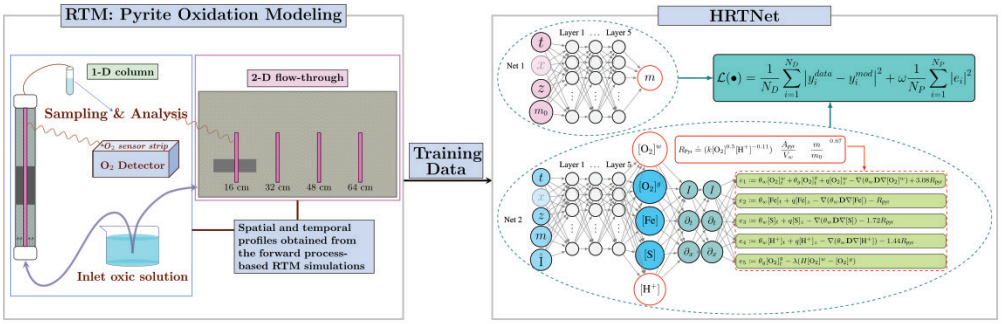

Figure 1 *Schematic diagram of the problem setup and overall workflow of the proposed surrogate modeling approach. The left panel displays exemplary reactive transport systems involving 1-D and 2-D flow-through setups by Battistel* et al. *(2019). The right panel is the surrogate model architecture showing its learning mechanism.*

training data fed into the HRTNet (Fig. 1, right panel). The RTM process relies on the chemical reaction:

$$FeS_{1.72} + 3.08O_2 + 0.72H_2 \rightarrow Fe^{2+} + 1.72SO_4^{2-} + 1.44H^+ \quad (1)$$

where Fe^{2+}, SO_4^{2-}, and H^+ are the main released oxidation products, implying O_2 consumption and acidity generation. Pyrite oxidation was simulated as kinetically controlled reactions with the rate law proposed by Williamson and Rimstidt (1994):

$$R_{pyr} = (k[O_2]^{0.50}[H^+]^{-0.11})\left(\frac{A_{pyr}}{V_w}\right)\left(\frac{m}{m_0}\right)^{0.67}(1-\Omega_{pyr}) \quad (2)$$

According to the chemical reactions and the rate law, the governing mass conservation equations for reactive transport in 1-D and 2-D flow-through systems are expressed as:

$$\theta_w \frac{\partial c_{w,i}}{\partial t} + \theta_g \frac{\partial c_{g,i}}{\partial t} + \mathbf{q}\cdot(\nabla c_{w,i}) - \nabla\cdot(\theta_w \mathbf{D}_i \nabla c_{w,i}) = -\sum_{j=1}^{N_j} v_{ij} R_j \quad (3)$$

$$\theta_g \frac{\partial c_{g,i}}{\partial t} = \lambda(H c_{w,i} - c_{g,i}) \quad (4)$$

where H (= 31.25) is Henry's coefficient for oxygen. Note that a mass transfer term taking into account the exchange of oxygen between the aqueous and gaseous phases was considered in the transport equations to account for the effect of entrapped gas bubble in the porous media. We integrate the pyrite reaction law and the governing PDEs into the neural networks by designing a tailored two-network architecture (Net 1 and Net 2) shown in Fig. 1 (right panel). HRTNet aims to learn a mapping $f(t, \boldsymbol{x}, m_0) \rightarrow c$, where $\boldsymbol{x}$ is a spatial vector with component z for the 1-D column and x, z for the 2-D flow-through system. m_0 is the initial pyrite concentration, which is zero in the purely sandy media where pyrite is absent, and c represents the target concentrations. This architecture ensures that HRTNet approximates f and adheres to the underlying chemical and physical laws.

Net 1 is a pure data-driven network that outputs the pyrite concentration, m, which acts as one of the inputs of Net 2, and is used in the pyrite reaction rate calculations. The input layer of Net 2 contains an extra variable I^0, an identifier to disambiguate where pyrite is absent when multiple training datasets are used. Net 2 first predicts the target concentrations. R_{pyr} is subsequently calculated by m, $O_2]^w$ and $[H^+]$, which is further used in calculating the PDE residuals obtained with the help of automatic differentiation to construct the loss function. The two networks interplay with each other by minimizing the loss. Thus, HRTNet incorporates the chemistry- and physics-informed learning in a flexible way to capture the spatial and temporal dynamics with various initial pyrite concentrations. The half-transparent neuron x in both networks (Fig. 1) allows identifying between 1-D and 2-D cases. Table 1 lists the parameters with their values used to calculate the PDE residuals for 1-D and 2-D flow-through setup.

Results

We trained HRTNet based on the results of the forward process-based reactive transport simulations in 1-D and 2-D systems. In 1-D column, the training data consists of four datasets with various initial

Table 1 Parameters and their values used in the PDE residuals of HRTNet in 1-D and 2-D flow-through setup.

Parameter	Description	1-D column	2-D flow-through
θ_w [-]	Volumetric water content	0.347	0.358
θ_g [-]	Volumetric gas content	0.033	0.022
q [m/s]	Specific discharge	6.03×10^{-6}	6.60×10^{-6}
D [m²/s]	Dispersion coefficient	2.50×10^{-9}	4.41×10^{-9}; $1.02 \times 10^{-9\#}$
λ [1/s]	Mass transfer coefficient	1.95×10^{-6}	4.26×10^{-6}

#The first and second value refers to the longitudinal and transverse dispersion coefficients respectively

pyrite concentrations, [30; 45; 60; 75] mol/L_{water}. Fig. 2 compares HRTNet prediction results and the process-based simulation at different reaction hours with an initial pyrite concentration of 52 mol/L_{water}, which was not part of the training data.

HRTNet performs consistently with RTM in all cases considering the prediction of dissolved oxygen O_2^w, oxygen concentration in the gaseous phase O_2^g and remaining pyrite concentration. Slight discrepancies between HRTNet and RTM in iron, sulfur, and proton profiles after the reaction zone can be observed, especially at early time (t = 3.2 *h* in Fig. 2). Overall, HRTNet can accurately capture the spatiotemporal dynamics with varying initial pyrite concentrations, a remarkable achievement among the existing DL-based surrogate models. This strong performance stems from HRTNet's flexible and generalized learning mechanism. Its two-network structure effectively integrates governing physics and chemistry principles, enabling HRTNet to achieve outstanding predictions beyond the training conditions.

Similarly, in the 2-D flow-through case, HRTNet was trained on training data consisting of multiple datasets from RTM, with initial pyrite concentrations, [10; 20; 30; 40] mol/Lwater. Fig. 3 compares the HRTNet's predictions on the second row with ground truth from RTM on the first row.

The initial pyrite concentration is 33.82 mol/L_{water}, the same as in the experimental setup. The outstanding agreement demonstrates that HRTN*et also* performs very well in 2-D flow-through.

Conclusion

The proposed HRTNet approach systematically integrates the governing chemical and physical equations with neural network architecture to allow transport and geochemistry-aware learning. The model relies on a flexible architecture based on two networks sharing a common loss function, allowing the incorporation of data-driven and physics-chemistry-informed contributions.

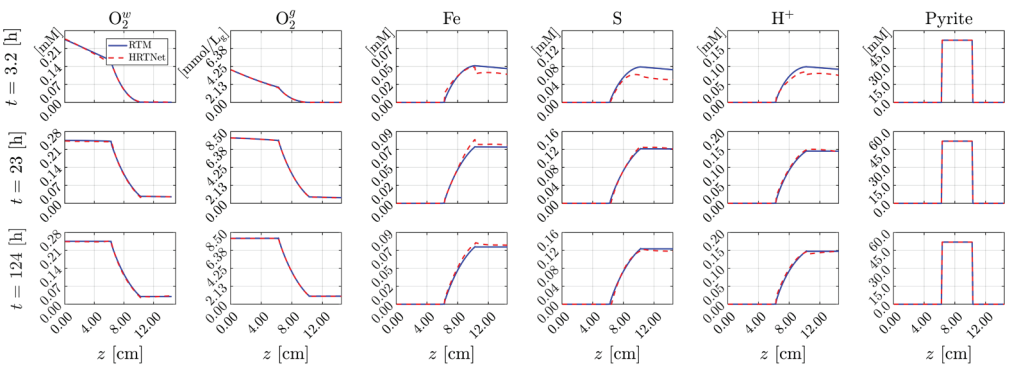

Figure 2 Comparison between HRTNet predictions and RTM simulations with initial pyrite concentration of 52 mol/L_{water} in 1-D column setup. Blue lines show ground truth from RTM simulations and the red dashed lines present the predictions obtained from the intelligent surrogate model.

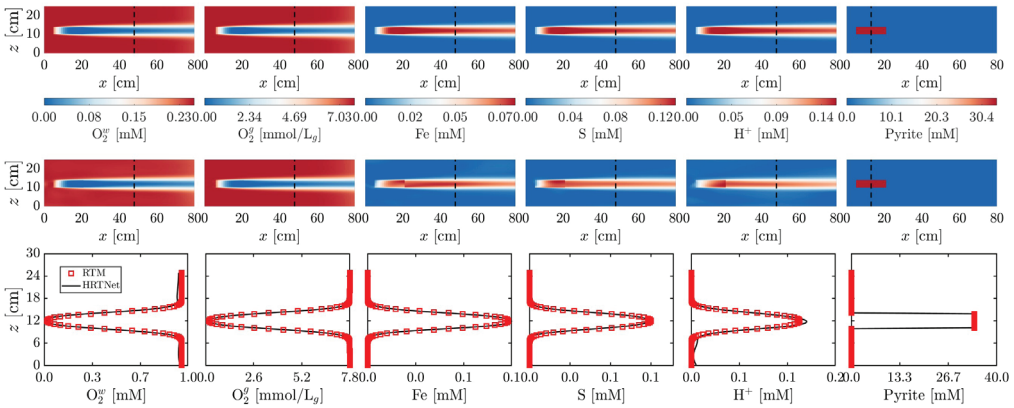

Figure 3 *HRT Predictions in 2-D flow-through chamber at t=50 h: top row – RTM, middle row – HRTNet, bottom row – vertical profiles at x = 13 cm for pyrite and x = 48 cm for others. The black dashed lines represent the cross section where oxygen sensor is placed at x = 48 cm, except for pyrite for which profile at x=13 cm is shown: the corresponding results are on the third row. The red squares represent ground truth from RTM and the black lines are the predictions of HRTNet.*

The two components can effectively capture the data patterns and the reactive transport dynamic features.

We considered examples including pyrite oxidation in 1-D and 2-D geochemically heterogeneous domains to evaluate HRTNet's performance. The results reveal that the predictions obtained by the trained surrogate model agree well with those from mechanistic RTMs. Furthermore, the physics- and chemistry-informed learning was promising to achieve a good generalization capability, because HRTNet could predict the desired spatio-temporal dynamics for a wide range of initial concentrations beyond the training datasets. Based on these encouraging results, the proposed approach could be extended to more complex systems in which not only pyrite oxidation but also other reactive processes control the formation of acid mine drainage.

Acknowledgements

This study is funded by Jane and Aatos Erkko Foundation (grant no. 220021). This work has also been supported by the Research Council of Finland (Finnish Centre of Excellence of Inverse Modeling and Imaging), Flagship of Advanced Mathematics for Sensing Imaging and Modelling (grant no. 358944), and the Research Council of Finland project 321761. M.M. acknowledges the support from the Research Council of Finland through HiFi-MuTaNTS (grant no. 364773) project. Finally, the authors thank the IT Center for Science, Finland (CSC), for generously sharing their computational resources.

References

Battistel M, Muniruzzaman M, Onses F, Lee J, Rolle M (2019) Reactive fronts in chemically heterogeneous porous media: Experimental and modeling investigation of pyrite oxidation. Applied Geochemistry 100: 77–89

Battistel M, Stolze L, Muniruzzaman M, Rolle M (2021) Arsenic release and transport during oxidative dissolution of spatially-distributed sulfide minerals. J Hazardous Materials 409: 124651

Chandra AP, Gerson AR (2010) The mechanisms of pyrite oxidation and leaching: A fundamental perspective. Surface Science Reports 65(9): 293–315

De Lucia M (2024) DecTree: a physics-based geochemical surrogate for surface complexation of uranium on clay. Advances in Geosciences 65: 45–54

De Lucia M, Kühn M (2021) DecTree v1.0 – chemistry speedup in reactive transport simulations: purely data-driven and physics-based surrogates. Geoscientific Model Development 14: 4713–4730

Degen D, Cacace M, Wellmann F (2022) 3D multi-physics uncertainty quantification using physics-based machine learning. Scientific Reports 12: 17491.

Degen D, Caviedes Voullième D, Buiter S, Hendricks Franssen HJ, Vereecken H, González-Nicolás A, Wellmann F (2023) Perspectives of physics-based machine learning strategies for geoscientific applications governed by partial differential equations. Geoscientific Model Development 16(24): 7375–7409

Demirer E, Coene E, Iraola A, Nardi A, Abarca E, Idiart A, de Paola G, Rodríguez-Morillas N (2023) Improving the performance of reactive transport simulations using artificial neural networks. Transport in Porous

Media 149: 271–297

Guérillot D, Bruyelle J (2020) Geochemical equilibrium determination using an artificial neural network in compositional reservoir flow simulation. Computational Geosciences 24: 697–707

Jatnieks J, De Lucia M, Dransch D, Sips M (2016). Data-driven surrogate model approach for 733 improving the performance of reactive transport simulations. Energy Procedia 97: 447–453

Kefeni KK, Msagati TAM, Mamba BB (2017) Acid mine drainage: Prevention, treatment options, and resource recovery: A review. J Cleaner Production 151: 475–493

Leal AMM, Kyas S, Kulik DA, Saar MO (2020) Accelerating reactive transport modeling: on-demand machine learning algorithm for chemical equilibrium calculations. Transport in Porous Media 133: 161–204

Laloy E, Jacques D (2022) Speeding up reactive transport simulations in ce- ment systems by surrogate geochemical modeling: Deep neural networks and k-nearest neighbors. Transport in Porous Media 143: 433–462

Li Y, Lu P, Zhang G (2022) An artificial-neural-network-based surrogate modeling workflow for reactive transport modeling. Petroleum Research 7(1): 13–20

Liu XY, Zhu M, Lu L, Sun H, Wang JX (2024) Multi-resolution partial differential equations preserved learning framework for spatiotemporal dynamics. Communications Physics 7:31

Marcato A, Santos JE, Boccardo G, Viswanathan H, Marchisio D, Prodanović M (2023) Prediction of local concentration fields in porous media with chemical reaction using a multi scale convolutional neural network. Chemical Engineering Journal 455: 140367

Moeini F, Ershadnia R, Rubinstein RL, Versteeg R, Li P, McGarr JT, Meyal A, Wallace CD, Dai Z, Carroll KC, Soltanian MR (2024) Employing generative adversarial neural networks as surrogate model for reactive transport modeling in the hyporheic zone. J Hydrology 639: 131485

Moncur MC, Jambor JL, Ptacek CJ, Blowes DW (2009) Mine drainage from the weathering of sulfide minerals and magnetite. Applied Geochemistry 24(12): 2362–2373

Muniruzzaman M, Pedretti P (2021). Mechanistic models supporting uncertainty quantification of water quality predictions in heterogeneous mining waste rocks: a review. Stochastic Environmental Research and Risk Assessment 35 (5): 985-1001.

Prasianakis NI, Haller R, Mahrous M, Poonoosamy J, Pfingsten W, Churakov SV (2020) Neural network based process coupling and parameter upscaling in reactive transport simulations. Geochimica et Cosmochimica Acta 291: 126–143

Raissi M, Perdikaris P, Karniadakis GE (2019) Physics-informed neural networks: A deep learning framework for solving forward and inverse problems involving nonlinear partial differential equations. J Computational Physics 378: 686–707

Raissi M, Yazdani A, Karniadakis GE (2020). Hidden fluid mechanics: Learning velocity and pressure fields from flow visualizations. Science 367: 1026–1030

Rao C, Ren P, Wang Q, Buyukozturk O, Sun H, Liu Y (2023). Encoding physics to learn reaction–diffusion processes. Nature Machine Intelligence 5: 765–779

Simate GS, Ndlovu S (2014) Acid mine drainage: Challenges and opportunities. J Environmental Chemical Engineering 2(3): 1785–1803

Sprocati R, Rolle M (2021) Integrating process-based reactive transport modeling and machine learning for electrokinetic remediation of contaminated groundwater. Water Resources Research 57: e2021WR029959

Sprocati R, Guadagnini A, Ceresa L, Gallo A, Rolle M (2025) Global sensitivity analysis of mass transfer and reaction dynamics for electrokinetic transport in porous media. Advances in Water Resources doi.org/10.1016/j.advwatres.2025.104887

Steefel CI (2019) Reactive transport at the crossroads. Reviews in Mineralogy and Geochemistry 85: 1–26

Steefel CI, DePaolo DJ, Lichtner PC (2005) Reactive transport modeling: An essential tool and a new research approach for the earth sciences. Earth and Planetary Science Letters 240: 539–558

Williamson MA, Rimstidt J (1994) The kinetics and electrochemical rate-determining step of aqueous pyrite oxidation. Geochimica et Cosmochimica Acta 58, 5443–5454

Xu TF, White SP, Pruess K, Brimhall GH (2000) Modeling of Pyrite Oxidation in Saturated and Unsaturated Subsurface Flow Systems. Transport in Porous Media 39: 25–56

Yu Z, Dai H, Yang J, Zhu Y, Yuan S (2024) Global sensitivity analysis with deep learning-based surrogate models for unraveling key parameters and processes governing redox zonation in riparian zone. J Hydrology 638: 131442